IJASRM

International Journal of Advanced Scientific Research and Management, Volume 3 Issue 10, Oct 2018

www.ijasrm.com

ISSN 2455-6378

Synthesis and dielectric relaxations in self-assembled Cadmium Sulphide nanorods dispersed in conducting polymer

Kousik Dutta

Department of Physics, Behala College, Parnasree;
Kolkata, West Bengal, Lndia

Abstract

Complex impedance and dielectric permittivity of Cadmium Sulphide-conducting polyaniline nanocomposite have been investigated as a function of frequency and temperature at different compositions. Inorganic-organic hybrid nanocomposites are synthesized by dispersing nanosized CdS in the conducting polyaniline matrix. Grain and grain boundary contributions are observed in the impedance spectra. The results are interpreted in terms of two series connected equivalent circuit. The dielectric permittivity 6200 is found for the for the sample with highest content of CdS nanoparticles. Large value of permittivity is well described described by Maxwell-Wagner polarization. Broad and asymmetric dielectric spectra are analyzed by Harviliak – Nigami relaxation function.

Keyword : *CdS nanorod, Conducting Polymer, Nanocomposites, Dilectric properties*

1. Introduction:

Nanostructure materials have gained special interest in the recent years due to their novel properties providing the new ideas in physics to explain it. Starting from the zero dimensional nanoparticles various structure such as nanoparticles, nanowires, nanorods, nanotubes have been produced from different materials. Because of their unique size tunable chemical and physical properties semiconductor nanomaterial have attracted much interest during the past two decades **(** Allivisator, 1996**)**. Among these, nanoparticles of II-IV semiconductors prepared as colloids have shown large emission quantum yields and thus have received considerable attention for optoelectronic applications (Brus, 1986). CdS is one of the widely studied material, plays an important role in optoelectronic device such as laser, light emitting diodes and solar cells. In recent years, CdS nanowires, nanoribbons, nanorods, nanotubes, and hollow microspheres have been synthesized by different methods such as template guided synthesis **(** Bawendi et al, 1990 and Bret et al, 2004**)**, hydrothermal method **(** Zhang et al, 2002), surfactant assisted growth **(** Zhao et al, 2003) sonochemical synthesis **(** Zhou et al, 2003), solvothermal route **(** Xau et al, 2005 and Zhang et al 2003 **)** sol-gel **(**Mathieu et al, 1995**)**, physical vapor deposition **(** Wu et al 2002) and electrochemical induced deposition(Xu et al 2000). In addition, Qian et al **(** Zhan et al 2000) reported a polymer controlled growth of CdS nanowires. To control the growth of the nanoparticles organic stabilizer (polymer) e.g polyethylene oxide(PEO) poly N- Vinyl 2 pyrolidone (PVP) polyvinylenabazle (PVK) are added during the wet chemical synthesis for capping the surface of the particle.

IJASRM

International Journal of Advanced Scientific Research and Management, Volume 3 Issue 10, Oct 2018

www.ijasrm.com

ISSN 2455-6378

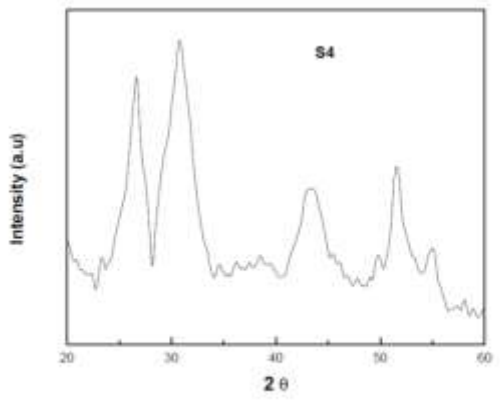

FIG. 1: X-ray diffraction pattern of CdS-PANI nanocomposites sample S4.

The shape plays an important role in determining the electronic properties of nanomaterials. CdS nanocrystals are dispersed in the polymer matrix to design organic-inorganic hybrid nanocomposites. The host polymer assists the assemble of CdS nanoparticles to form a new material with a deviation of spherical shape.

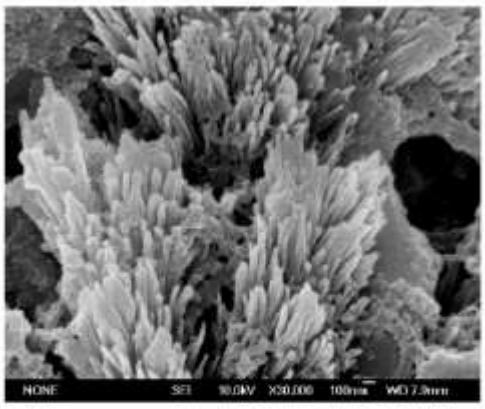

FIG. 2: Scanning Electron Micrograph (SEM) of nanocomposite sample S4.

Wire like assemblies of CdS nanoparticles are fabricated within core-shell cylindrical polymer brushes. (Zhang et al, 2004) Composites of CdS nanoparticles incorporated in polyurea (Hirai et al, 1999) and sulfonated polystyrene **(** Du et al, 2002) have been prepared. Conducting polymers are very useful supporting medium for the electrical characterizations of nanostructured systems. Polyaniline (PANI) is one of the most studied conducting polymer because of its good electrical conductivity, environmental stability and relative easy synthesis. (Skotheim et al, 1998) In the present work, synthesis of nanosized CdS have been prepared in the presence of conducting polyaniline (PANI). Extensive research activities on PANI have been performed because of high electrical conductivity. (Skotheim et al, 1998) Electrical properties of conducting polymers primarily depend on the preparation condition. The presence of inorganic nanomaterials strongly influences the electronic properties of polymer. Moreover, the integrating properties of inorganic material and polymer give rise to composites with different physical property.

Recently the physical properties of nanomaterials are extensively investigated for potential technological application and to understand the nanoscience. Nanomaterials have two distinct microstructures (i) nonocrystalline grain and (ii) surface and interface (grain boundary) components. The large number of surface and interfaces affect drastically the physical properties of materials. Semiconducting nanomaterials exhibit a very high resistance due to interface effect. Impedance spectroscopy is a powerful tool to distinguish the grain and grain boundary effects in complex system. In this work it is investigated that the electrical and dielectric properties of nanosiized CdS in the presence of Pani. Measurement of ac conductivity have been extensively used to understands the conduction process various models such as quantum mechanical tunneling model (QMT) small polaron tunneling model (SPTM), large polaron tunneling model (LPTM) atomic hopping model and the correlated barrier hopping model (CBH) have been proposed to explain the ac conduction mechanism for different materials. In this paper the temperature and frequency dependence of ac conduction and dielectric properties were measure for CdS pani nanocomposite.

2. Experimental:

Synthesis of a material is a vital part of material research, because proper tailoring is necessary to make a material interesting in properties. Of the different methods of preparation, chemical method of preparation of nanomaterial is more

advantageous because of good control over stoichiometry of the reactants is obtained. In this research work all the chemicals used were of analytical grade. Aniline and ammonium peroxydisulphate (APS) ($(NH_4)_2S_2O_8$) were obtained from E. Merck (India). Aniline (AR grade) was purified and stored at -15^0C in a refrigerator prior to use. APS oxidant was used as received.

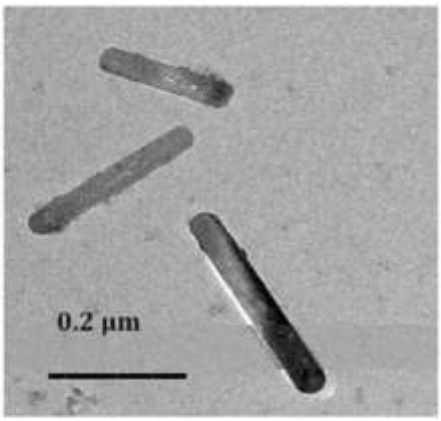

FIG. 3: Transmission Electron Micrograph (TEM) of nanocomposite sample S4.

CdS nanoparticle were synthesized by a standard chemical technique. (Trindade et al, 2001) In a typical synthesis 1.35 gm of cadmium chloride ($CdCl_2$) was dissolved in 500 ml of deionized water and stirred for 1 hour at room temperature. Aqueous solution of thioglycerol (15mM) was mixed drop wise with the aqueous solution of cadmium chloride under constant stirring. The pH of the resultant solution was kept at 10 with the addition of ammonium hydroxide aqueous solution. After 45 minutes Na_2S solution was mixed with the above reaction mixture and stirred for 3 hours at 50^0 C. Finally the resultant nanoparticles were washed with deionized water several times to remove the unwanted impurities and dried in a vacuum oven at 60^0 C.

The required quantity of CdS nanoparticle was ultrasonically dispersed in 40 ml deionized water. Aniline monomer of known volume was slowly added into the dispersion under sonication at room temperature. Then the aqueous solution of APS maintaining aniline : APS mole ratio of 1:1.25 was added drop wise with the previous solution. After few hours the resulting solution was turned into green color which indicates the formation of polyaniline. The solution was then kept under sonication for about 6 hours to ensure complete polymerization. Finally the resulting green dispersion was centrifuged. The resulting nanocomposites were washed thoroughly with distilled water for several times. Different compositions of nanocomposite samples by varying the amount of aniline (polyaniline) were prepared as shown in Table I. The samples were pressed into pellets of diameter 1 cm. The thickness of the samples varies from 0.08 cm to 0.12 cm.

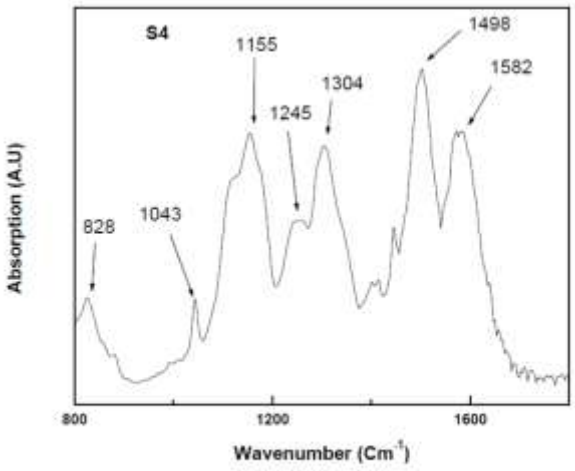

FIG. 4: Fourier Transform Infrared (FTIR) spectra of sample S4.

The phase identification of the nanocomposites sample were performed using a Philips Difractrometer (PW1710) with Cu k_α radiation in 2 θ range from to 20 to 60^0. Scanning electron microscope (SEM)(Model JEOL JSM6700F) image was obtained using scanning electron microscope. Infrared spectra of the nanocomposite samples palletized with KBr were performed by Fourier transformed spectrometer (Perkin-Elmer model 1600). The temperature dependent capacitance (C) and dielectric loss factor (D) were measured by Agilent 4192 Impedance Analyzer. The electrical contacts were made by silver paint on both sides of the sample.

IJASRM

International Journal of Advanced Scientific Research and Management, Volume 3 Issue 10, Oct 2018

www.ijasrm.com

ISSN 2455-6378

3. Results and discussion:

Figure 1 displays the powder X-ray diffraction (XRD) of the sample S4. The spectrum of pure PANI shows no characteristics peak (not shown in this manuscripts), only a hump near 25^0 is obtained. Thus polyaniline is amorphous in nature. The hump at 25^0 is for regular repetation of aniline monomer. The characteristic peaks at angles (2θ) of 26.5, 30.8, 43.7, 51.9, 54.9 which are due to Bragg's reflections from 111, 200, 220, 311 and 222 planes of nanocrystalline CdS. It (CdS) exists in two crystalline phases, cubic zincblende and hexagonal wurtzite. The present XRD pattern matches well with the reported cubic phase of CdS [Joint Committee on Powder Diffraction Standards (JCPDS) No. 42-1411]. The peaks are fairly broad suggesting the nanostructure of CdS.

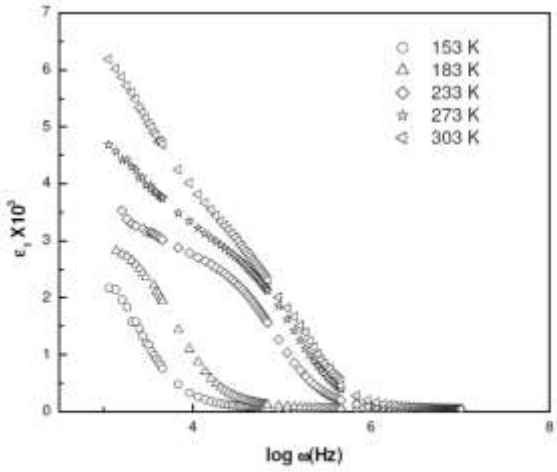

FIG. 5: Frequency dependence of the real part of relative dilectric constant (ε_1) at different temperatures for the sample S4.

The scanning electron micrograph (SEM) of the nanocomposite sample S4 is shown in Figure 2. Rod like morphology of CdS is observed in the micrograph. The nanorods are aligned and have almost the same width. The most surprising fact is that CdS nanoparticles are assembled in one dimensional pattern in the presence of polyaniline matrix.

Transmission electron microscopy (TEM) images of S4 are depicted in Figure 3. The CdS nanorods are uniform diameter of about 40 nm. The length of nanorods varies from 200 nm to 400 nm. The aspect (Length/Diameter) of nanorods is in the range of 5-10 nm.

A typical FTIR spectrum of the nanocomposite sample S4 is illustrated in Figure 3. The bands at 1582 and 1498 cm^{-1} are ttributed to C=N and C=C stretching mode of vibration for the quinonoid and benzenoid units of polyaniline. The appearance of characteristics absorption and around 1245 cm^{-1} is related to the C-N stretching in bipolaron structure. These results indicate that the polymer is highly doped and exists in conducting emeraldine salt form. The peaks at 1304 cm^{-1} corresponds to C-N stretching of secondary amine in polymer main chain and clearly seen in these sample. The bands in the region 1000 – 1200 cm^{-1} are due to in plane bending vibration of C-H mode. The band at 828 cm^{-1} originates out of plane C-H bending vibration. The typical FTIR spectrum of PANI is consistent with the previous results. (Stejskal et al 1998 and Quillard et al, 1994) Almost all the bands reveal blue shift in the nanocomposites which indicates that there is a strong interaction between polyaniline and CdS nanoparticles.

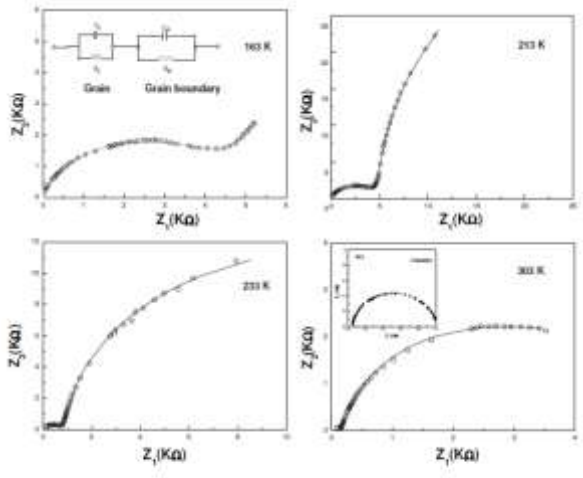

FIG. 6: Impedance spectra of the sample S4 at four different temperatures. The solid lines are fits to the proposed equivalent circuit for the sample. Inset represents the impedance spectra of pure polyaniline at room temperature.

IJASRM

International Journal of Advanced Scientific Research and Management, Volume 3 Issue 10, Oct 2018

www.ijasrm.com

ISSN 2455-6378

The frequency dependent dielectric permittivity of a solid arises due to different reasons some of them are as follows (1) displacement of ionic charge with respect to their nuclei in the material (2) displacement of ions from their equilibrium positions and (3) dipolar contribution. Out of these three main contribution only dipolar contribution shows the frequency and temperature dependence at low temperature. Capacitance and dissipation factor were measured within a frequency range 20 Hz to 10 MHz and in the temperature region in between 77 K to 300 K. Real part of complex dielectric function (ε_1) was determined by considering the geometry of parallel plate capacitor formed by silver paint, The real and imaginary part of the dielectric constant can be calculated from the relation $\varepsilon_1 = Cd/A\ \varepsilon_0$. d is thickness and A is area of sample and ε_0 is the vacuum dielectric constant. The imaginary component of dielectric constant, ε_2 was obtained from $\varepsilon_2 = \varepsilon_1 D$. Complex impedance Z was calculated from the relation, $Z = 1/(i\omega C_0 \varepsilon)$, where $C_0 = \varepsilon_0 A/d$ is the geometrical capacitance and ω is angular frequency. The dielectric constant ε_1 as a function of frequency for different temperature are presented for S4 sample in Figure 4. The magnitude and frequency dependence of ε_1 are strongly dependent on the nanosized CdS content. It is observed fact from the figure 4 that the variation of the real part of dielectric permittivity with frequency at constant different temperature that the dielectric permittivity is strongly dependent on frequency at lower frequency region, where ε_1 decreases with increasing frequency and the variation is enhanced at higher temperature than the lower temperature. However, a nearly frequency independent behavior has been observed at higher frequency > 1 MHz. This is because, the dipoles at lower temperature are freeze and the polarization decayed for these reason a sharp decrease in ε_1 has been observed at lower frequency.

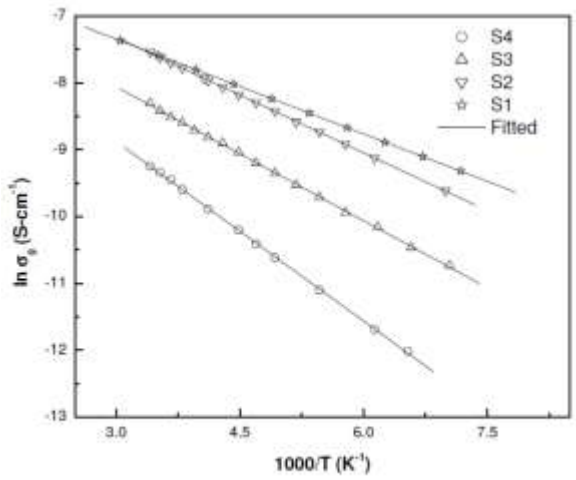

FIG. 7: Arrhenius plot of grain conductivity for the four different samples.

This type of behavior has been observed in those samples which have different permittivity and conductivity region. The dielectric permittivity of such an inhomogeneous system can be analysed by Maxwell-Wagner capacitor model (Maxwell, 2009, Catalan, et al, 2000, Hippel, 1954). An exceptionally high value of about 6200 is found for the sample with highest content of CdS. In case of more conducting sample S1, ε_1 reduces to about 2300. The maximum value of dielectric constant of bulk CdS is about 8.9. The present observation of ε_1 is remarkable as it is larger than the constituent material by three orders of magnitude.

IJASRM

International Journal of Advanced Scientific Research and Management, Volume 3 Issue 10, Oct 2018

www.ijasrm.com

ISSN 2455-6378

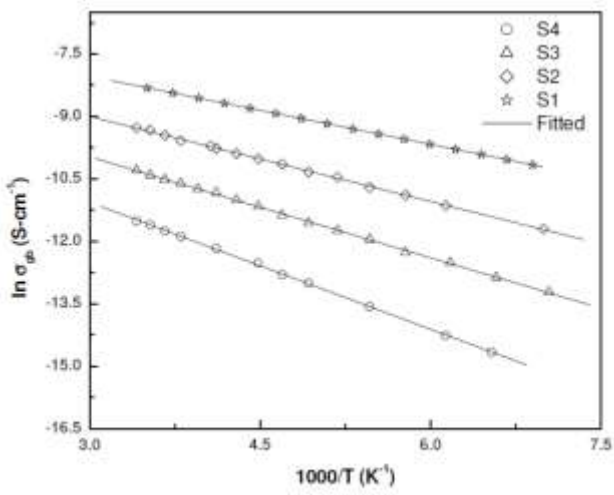

FIG. 8: Arrhenius plot of grain boundary conductivity for the different samples.

Figure 5 represents the complex impedance, $Z=Z_1 +iZ_2$ plots for the sample S4 at different temperatures. At room temperature, two incomplete semicircles are observed. The high frequency contribution dominates with lowering of temperature. The features of the impedance spectra of polycrystalline composite materials primarily depend on the microstructure. The nanocomposite samples consist of nanometer size grains which introduce more grain boundaries within the samples. The impedance spectra can be interpreted by the equivalent circuit consisting of series connected parallel resistance (R) and capacitance (C) components as shown in Fig.5. The position of the maximum arc in the impedance diagram is determined by the relation ω_{max} RC = 1, where $\omega_{max} = 2\pi f$, f is the applied frequency. The larger values of R and C at grain boundary lead to smaller ω_{max} compared to grain. Moreover, ω_{max} lies outside the available frequency range and only some portions of semicircles are obtained at higher temperature.

The grain and grain boundary responses are analyzed by the following relations

$$Z_1 = \frac{R_g}{1+(\omega R_g C_g)^2} + \frac{R_{gb}}{1+(\omega R_{gb} C_{gb})^2} \quad (1)$$

$$Z_2 = R_g\left[\frac{\omega R_g C_g}{1+(\omega R_g C_g)^2}\right] + R_{gb}\left[\frac{\omega R_{gb} C_{gb}}{1+(\omega R_{gb} C_{gb})^2}\right] \quad (2)$$

where (R_g, R_{gb}) and (C_g, C_{gb}) are resistance and capacitance of grain and grain boundary respectively. Equations (1) and (2) represent two ideal semicircles whose centers lie on the real Z_1 axis. The constant phase elements (CPE) capacitors $C(\omega) = B(i\omega)^{n-1}$ are assumed to analyze the more attuned semicircles(Macdonald, 1987 and Jonscher, 1983). The parameter B is constant for a given set of experimental data. The exponent n varies between 0 and 1. The impedance of CPE behaves as an ideal capacitor for n = 1 and ideal resistor for n = 0. The experimental data are best fitted employing complex nonlinear curve fitting LEVM program developed by Macdonald. The solid lines in Figure 5 represent the best fitted calculated values. Both C_{gb} and C_g are weak temperature dependent.

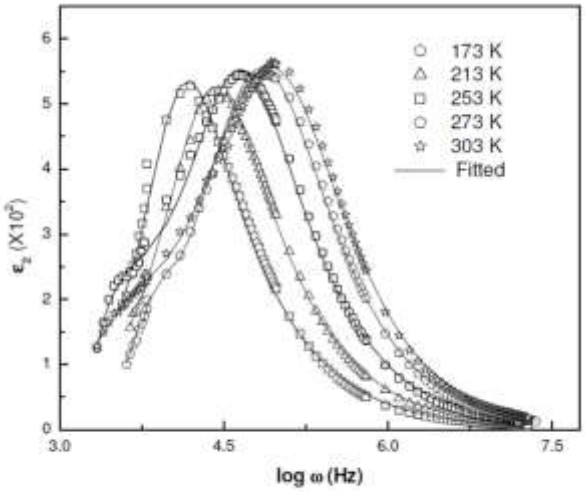

FIG. 9: Frequency dependence of imaginary component of dielectric constant (ε_2) at selected temperatures for the sample S4. The solid lines are fits to Eq.4.

Contribution of grain and interfacial boundary resistance and capacitance may give information about the transport process in the composite samples. It is observed that the interfacial boundary resistance is much greater than that of grain resistance which indicates interfacial boundary contribution dominated over the grain contribution in these composite samples. This type of conduction process can explained by the hopping mechanism, where the carrier mobility is dominated by a factor that increases with rise of temperature exponentially. This

temperature dependent factor is determined by thermal activation in order to overcome the potential barrier between the sites by hopping. Grain (σ_g) and grain boundary (σ_{gb}) conductivities have been calculated from the best fitted values of R_g and R_{gb}. Figures 6 and 7 show the temperature dependence of grain and grain boundary conductivity. The estimated grain boundary conductivity is about 100 times lower than that of grain conductivity. Both σ_g and σ_{gb} follow Arrhenius type process with temperature as evidence from the plots in Figs. 6 and 7 and support the above explanation. The activation energies are derived from the slopes of the straight lines as shown in Table I. The activation energy of the grain interior is smaller than that of grain boundary. The conductivity of grain boundary region is mainly determined by the microstructure. The temperature dependence of conductivity of PANI obeys Mott's three dimensional variable range hopping process.(Skotheim et al, 1998) Thermally activated conductivity variation suggests that PANI is not dominating the conduction process. The unusually large dielectric constant can be explained by interfacial Maxwell-Wagner (MW) interfacial relaxation commonly applied in heterogenous system. The nanocomposites consist of conducting grains and resistive grain boundaries. Under the application of external electric field, the charge carriers can easily migrate the grains but are accumulated at the grain boundaries. This process can produce large polarization and high dielectric constant. The small conductivity of grain boundary contributes to high value of dielectric constant at low frequency. The static dielectric constant based on the equivalent circuit in Figure 5 can be expressed as

$$\epsilon_1(0) = \frac{R_g^2 C_g + R_{gb}^2 C_{gb}}{C_0 (R_g + R_{gb})^2} \qquad (3)$$

Resistance and capacitance of grain boundary are much larger than that of grain. In MW polarisation, dielectric constant under such condition can be approximated from eq.(3) as $\varepsilon_1(0) = C_{gb}/C_0$. A large value of C_{gb} leads to very high value of dielectric constant. The ratio of CdS and PANI modifies the microstructure i.e. grain boundary capacitance. This may be the possible reason for different values of ε_1 for different compositions. The dielectric loss spectra ε_2 as a function of frequency for S4 are shown in Fig.8 for different temperatures. The relaxation peak in the measured frequency domain is appeared at room temperature. The positions of the peaks move to lower frequency with the decrease of temperature. The dielectric response has been analyzed by the most generalized Havriliak-Negami (HN) function (Havriliak èt al, 1967).

$$\epsilon^* = \epsilon_\infty + \frac{\epsilon_s - \epsilon_\infty}{(1 + (i\omega\tau)^\beta)^\alpha} \qquad (4)$$

where τ is the average relaxation time which is given at the frequency of maximum dielectric loss. The difference $\Delta\varepsilon = \varepsilon_s - \varepsilon_\infty$ is known as the dielectric relaxation strength. The parameter β describes the distribution of the relaxation time of the system. Debye relaxation is obtained for $\alpha = 1$ and $\beta = 1$. The parameters α and β ranging between 0 and 1 are symmetric and asymmetric broadening of dielectric spectra.

TABLE 1: Weight percentage of polyaniline (x), activation energy from grain boundary (E_{gb}) and grain (E_g) conductivity and activation energy E_τ of dielectric relaxation, real part of relative dielectric permittivity ($\varepsilon 1$) at room temperature (RT):

Sample	x	Egb (meV)	Eg (meV)	Eτ (meV)	ε1 (RT)
S1	80	48	41	39	2300
S2	65	60	50	49	3300
S3	50	72	58	57	4850
S4	35	89	79	80	6200

The solid lines in Fig.8 show that the experimental data are reasonably good fitted with the calculated value of HN function. The value of β is different from unity which implies non- Debye relaxation process. This parameter manifests that the dispersion has a broad distribution of relaxation time. The dielectric strength $\Delta\varepsilon$ increases with increase of temperature. The relaxation times, τ at different temperatures are obtained from the best fitted data to

eqn. (4). The Arrehenius plot (not shown in this manuscript) of ln τ against 1/T for the different samples suggest that the temperature variation of τ can be described by thermally activated Arrhenius law,

$$\tau = \tau_0 exp(E_\tau / kT) \qquad (5)$$

where τ_0 is the relaxation time at high temperature, E_τ is the activation energy of dielectric process and k is Boltzmann constant. The slope of the best fitted straight line gives the activation energy as shown in Table I. The most interesting fact is that the activation energies are in excellent agreement with the values obtained from grain conductivity.

4. Conclusion:

The growth and the assemble of CdS nanoparticles in the polymer matrix is a very complicated process. Dispersion of CdS nanoparticles into the conducting polyaniline makes the nanoparticle to form the the rod like assemblies. Actually this is happen because of the molecular level interaction between polyaniline and the CdS nanoparticles which may be the reasons for the formation of rods along the backbone of the polymer matrix. After chemical, PANI was coated onto the surface of CdS microspheres successfully . It was obvious that the light shelled structure PANI was successfully coated onto the surface of the spherical CdS. Polymer coated CdS nanoparticles then aligned to make CdS nanorod. (Yu et al, 2005). In these process interaction between thiol group and polymer plays major role to form the nanorod.

Impedance data demonstrate the existence of electrically semiconducting grains and more resistive grain boundaries. The values of dielectric constant exhibit large variations with compositions, temperature and frequency. The dielectric response is characterized by Maxwell-Wagner relaxation The variations of microstructure with compositions render different dielectric constants.

References:

[1] Allivisator, A. P. Semiconductor Clusters, Nanocrystals, and Quantum Dots. Science, 271 (5251), 933-937 (1996).
[2] Bawendi, M. G., Steigerwald, M. L. and Brus L.E., Annu. Rev. Phys. Chem. 41, 477 (1990).
[3] Bret J. S. Johnson, Johanna H. Wolf, Zalusky Andrew S. and Marc A. Hillmyer, Template Syntheses of Polypyrrole Nanowires and CdS Nanoparticles in Porous Polymer Monoliths. Chem. Mater, 16(15), 2909-2917 (2004).
[4] Brus, L. Electronic wave functions in semiconductor clusters: experiment and theory. J. Phys. Chem, 90 (12) , 2555-2560 (1986).
[5] Catalan G., NEill D.O., Bowman R.M., Gregg J.M., Relaxor features in ferroelectric superlattices: A Maxwell–Wagner approach. Appl. Phys. Lett.77, 3078 (2000)
[6] Du H., Xu G. Q. and Chin W. S., Synthesis, Characterization, and Nonlinear Optical Properties of Hybridized CdS−Polystyrene Nanocomposites. Chem. Mater. 14(10), 4473-4479 (2002).
[7] Havriliak S. and Negami S., A complex plane representation of dielectric and mechanical relaxation processes in some polymers. Polymer 8, 161 (1967)
[8] Hippel V., Dielectric and waves, 1954, Wiley: New York
[9] Hirai T., Watanabe T. and Komasawa I., Preparation of Semiconductor Nanoparticle−Polyurea Composites Using Reverse Micellar Systems via an in Situ Diisocyanate Polymerization J. Phy. Chem. B 103 (46), 10120-10126 (1999).
[10] Jonscher A. K., Dielectric Relaxation In Solids, 1983, Chesla Dielectric Group, UK
[11] Macdonald J. R., Impedance spetroscopy (John Wiley, New York,1987)
[12] Mathieu, H. Richard T., Allegre J., Lefebvre P. and Arnaud G. Quantum confinement effects of CdS nanocrystals in a sodium borosilicate glass prepared by the sol-gel process. J. Appl. Phys. 77(1), 287-293 (1995).
[13] Maxwell J.C., A Treatise on electricity and Magnetism, 2009, Oxford: Oxford university Press

[14] Quillard S., Louarn G., Lefrant S. and Macdiarmid A. G., Vibrational analysis of polyaniline: A comparative study of leucoemeraldine, emeraldine, and pernigraniline bases. Phys. Rev. B 50, 12496-12508 (1994).

[15] Skotheim T. and Elsenbaumer R., Handbook of Conducting Polymers, Marcel Dekker, New York, 1998

[16] Stejskal J., Sapurina I., Trchova M., Prokes J., Krivka I. and Tobolkova E., Solid-State Protonation and Electrical Conductivity of Polyaniline. Macromolecules 31(7), 2218-2222 (1998).

[17] Trindade T., Nanocrystalline Semiconductors: Synthesis, Properties, and Perspectives. Chem. Mater, 13(11), 3843 (2001).

[18] Wu X. C. and Tao Y.R. Growth of CdS nanowires by physical vapor deposition J. Cryst. Growth 242(3), 309-312 (2002).

[19] Xau D., Liu Z., Liang J. and Qian Y., Solvothermal Synthesis of CdS Nanowires in a Mixed Solvent of Ethylenediamine and Dodecanethiol. J. Phys. Chem. B, 109(30),14344-14349 (2005).

[20] Xu D., Xu Y., Chen D., Guo G., Gui L. and Tang Y., Adv. Mater. (Weinheim, Ger.)12, 520 (2000).

[21] Yu, J. H.; Joo, J.; Park, H. M.; Baik, S. I.; Kim, Y. W.; Kim, S. C.; Hyeon, T. Synthesis of quantum-sized cubic ZnS nanorods by the oriented attachment mechanism. J. Am. Chem. Soc. 2005, 127(15), 5662-5670.

[22] Zhang, H. Ma X., Jin Xu Y. Ji, , and Yang, D. Chem. Phys. Lett. 377, 654 (2002).

[23] Zhang, P. and Gao L., Synthesis and Characterization of CdS Nanorods via Hydrothermal Microemulsion Langmuir 19(1), 208-210 (2003).

[24] Zhan J., Yang X., Wang D., Li S., Xie Yi., Xia Y. and Qian Y., Polymer-Controlled Growth of CdS Nanowires Adv. Mater. 12(18), 1348-1351 (2000)

[25] Zhang M., Drechsler M. and Muller Axel. H. E., Template-Controlled Synthesis of Wire-Like admium Sulfide Nanoparticle Assemblies within Core−Shell Cylindrical Polymer Brushes. Chem. Mater, 16(3), 537-543 (2004).

[26] Zhao Q., Hou L., Huang R., and Li S., Surfactant-assisted growth and characterization of CdS nanorods. Inorg. Chem Commum, 6, 1459-1462 (2003).

[27] Zhou S., Feng Y. and Zhang L. Sonochemical synthesis of large-scale single crystal CdS nanorods. Matt. Lett, 57(19), 2936-2939 (2003)